

UC San Diego

UC San Diego Previously Published Works

Title

Controls on Millennial-Scale Atmospheric CO₂ Variability During the Last Glacial Period

Permalink

<https://escholarship.org/uc/item/14d642bt>

Journal

Geophysical Research Letters, 45(15)

ISSN

0094-8276

Authors

Bauska, TK
Brook, EJ
Marcott, SA
[et al.](#)

Publication Date

2018-08-16

DOI

10.1029/2018gl077881

Peer reviewed

Geophysical Research Letters

RESEARCH LETTER

10.1029/2018GL077881

Key Points:

- A new ice core record of carbon isotopes in atmospheric CO₂ suggests organic carbon sources controlled CO₂ during the last glacial period
- The millennial-scale CO₂ variability is tentatively linked to variations in Southern Ocean carbon sources
- Centennial-scale CO₂ variability during the last glacial period is associated with similarly abrupt changes during the deglaciation

Supporting Information:

- Supporting Information S1
- Supporting Information S2

Correspondence to:

T. K. Bauska,
tkb28@cam.ac.uk

Citation:

Bauska, T. K., Brook, E. J., Marcott, S. A., Baggenstos, D., Shackleton, S., Severinghaus, J. P., & Petrenko, V. V. (2018). Controls on millennial-scale atmospheric CO₂ variability during the last glacial period. *Geophysical Research Letters*, 45, 7731–7740. <https://doi.org/10.1029/2018GL077881>

Received 10 MAR 2018

Accepted 4 JUL 2018

Accepted article online 11 JUL 2018

Published online 10 AUG 2018

Controls on Millennial-Scale Atmospheric CO₂ Variability During the Last Glacial Period

T. K. Bauska¹ , E. J. Brook² , S. A. Marcott³ , D. Baggenstos⁴ , S. Shackleton⁴ , J. P. Severinghaus⁴ , and V. V. Petrenko⁵ 

¹Godwin Laboratory for Palaeoclimate Research, Department of Earth Sciences, University of Cambridge, Cambridge, UK, ²College of Earth, Ocean, and Atmospheric Sciences, Oregon State University, Corvallis, OR, USA, ³Department of Geoscience, University of Wisconsin-Madison, Madison, WI, USA, ⁴Scripps Institution of Oceanography, University of California, San Diego, La Jolla, CA, USA, ⁵Department of Earth and Environmental Sciences, University of Rochester, Rochester, NY, USA

Abstract Changes in atmospheric CO₂ on millennial-to-centennial timescales are key components of past climate variability during the last glacial and deglacial periods (70–10 ka), yet the sources and mechanisms responsible for the CO₂ fluctuations remain largely obscure. Here we report the ¹³C/¹²C ratio of atmospheric CO₂ during a key interval of the last glacial period at submillennial resolution, with coeval histories of atmospheric CO₂, CH₄, and N₂O concentrations. The carbon isotope data suggest that the millennial-scale CO₂ variability in Marine Isotope Stage 3 is driven largely by changes in the organic carbon cycle, most likely by sequestration of respired carbon in the deep ocean. Centennial-scale CO₂ variations, distinguished by carbon isotope signatures, are associated with both abrupt hydrological change in the tropics (e.g., Heinrich events) and rapid increases in Northern Hemisphere temperature (Dansgaard-Oeschger events). These events can be linked to modes of variability during the last deglaciation, thus suggesting that drivers of millennial and centennial CO₂ variability during both periods are intimately linked to abrupt climate variability.

Plain Language Summary Ice cores provide unique records of variations in atmospheric CO₂ prior to the instrumental era. While it is clear that changes in atmospheric CO₂ played a significant role in driving past climate change, it is unclear what in turn drove changes in atmospheric CO₂. Here we investigate enigmatic changes in atmospheric CO₂ levels during an interval of the last glacial period (~50,000 to 35,000 years ago) that are associated with abrupt changes in polar climate. To determine the sources and sinks for atmospheric CO₂, we measured the stable isotopes of carbon in CO₂ and found that the primary source of carbon to the atmosphere was an organic carbon reservoir. Most likely, this carbon was sourced from a deep ocean reservoir that waxed and waned following changes in either the productivity of the surface ocean or stratification of the deep ocean. We also found that atmospheric CO₂ can change on the centennial timescale during abrupt climate transitions in the Northern Hemisphere. This observation adds to a growing body of evidence that abrupt changes in atmospheric CO₂ are an important component of past carbon cycle variability.

1. Introduction

In order to predict the climate impacts of anthropogenic CO₂ emissions over the coming millennia (Clark et al., 2016), we must understand how the climate system and carbon cycle have interacted over these same timescales in the past. The CO₂ rise during the last deglaciation, arguably the most well-studied example of past carbon cycle variability, is likely a combination of millennial-scale climate change and glacial-interglacial shifts in temperature and ice volume, which are all amplified through a system of climate-carbon cycle feedbacks. To disentangle the millennial-scale component, we investigate carbon cycle variability of the last glacial period when climate variations were largely unaffected by changes in Northern Hemisphere insolation and ice volume that characterize glacial terminations (supporting information Figure S1).

During Marine Isotope Stage 3 (MIS3), atmospheric CO₂ varied between about 195 and 225 ppm with a roughly triangular waveform (Indermuhle et al., 2000; Figure 1e). This pattern mimics Antarctic temperature, rising during the strongest Antarctic warmings and falling during the coolings (Figure 1b). From the perspective of Greenland climate and the well-known Dansgaard-Oeschger (DO) events, CO₂ increases during cold

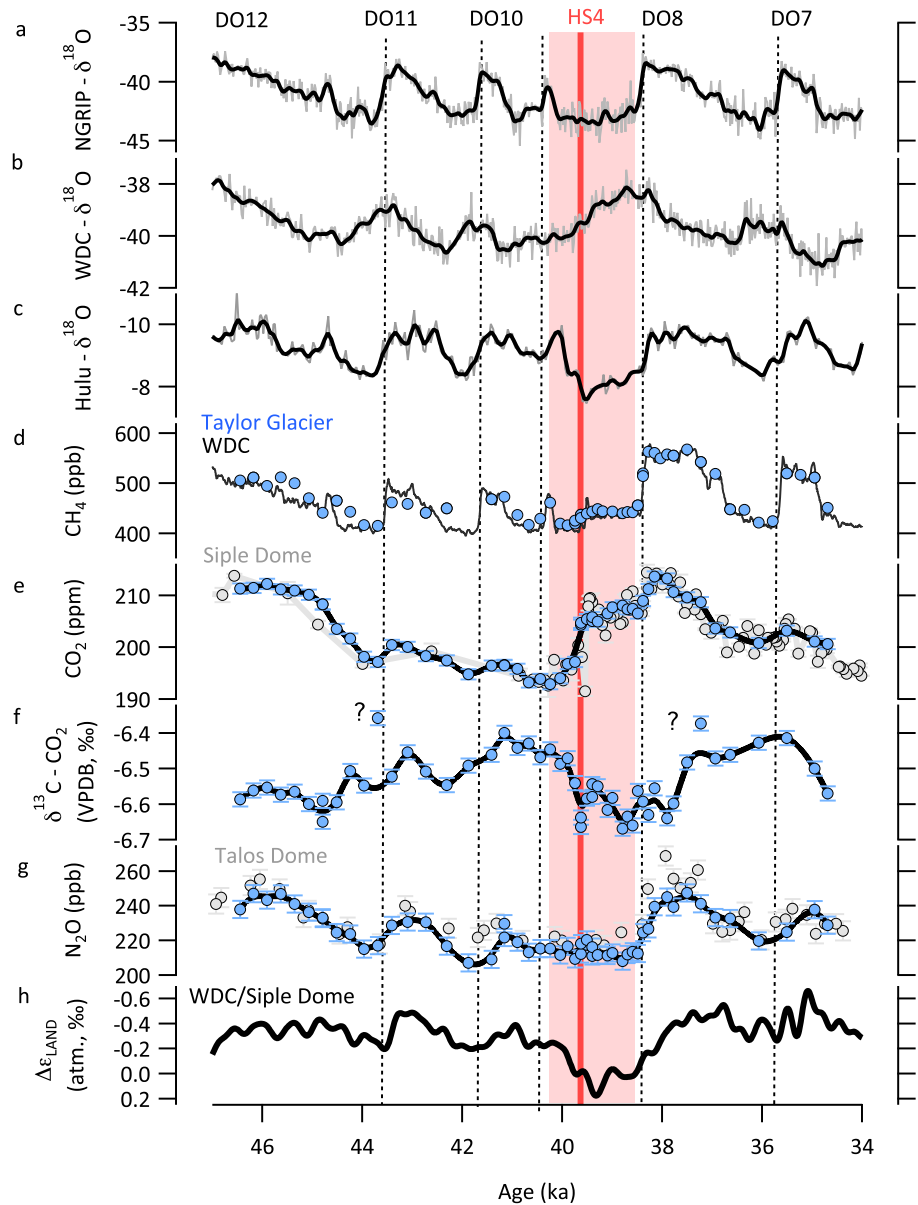


Figure 1. Taylor Glacier CO_2 , CH_4 , N_2O , and $\delta^{13}\text{C}-\text{CO}_2$ (blue markers with black smoothing spline; this study). (a) NGRIP $\delta^{18}\text{O}$ (North Greenland Ice Core Project Members, 2004). (b) WDC (WAIS Divide Ice Core) $\delta^{18}\text{O}$ (WAIS Divide Project Members, 2015). (c) Hulu Cave $\delta^{18}\text{O}$ (Cheng et al., 2016). (d) WDC (Rhodes et al., 2015; thin black line) and Taylor Glacier CH_4 . (e) Siple Dome (Ahn & Brook, 2014; gray markers) and Taylor Glacier CO_2 . (f) Taylor Glacier $\delta^{13}\text{C}-\text{CO}_2$. (g) Talos Dome (Schilt et al., 2010; gray markers) and Taylor Glacier N_2O . (h) Global Terrestrial O_2 isotopic fractionation, $\Delta\epsilon_{\text{LAND}}$, constrained from a combination of WDC and Siple Dome (Seltzer et al., 2017; Severinghaus et al., 2009). Dotted lines highlight the stadal to interstadial transitions, and the red bar highlights the Heinrich stadial with the associated rise in CO_2 and CH_4 and increase in $\Delta\epsilon_{\text{LAND}}$. The NGRIP chronology is increased by 0.63% prior to 22 ka for consistency with the WDC chronology (WAIS Divide Project Members, 2015).

phases (stadials; Ahn & Brook, 2008) with the most prominent increases corresponding to only those stadials associated with an enhanced flux of debris-laden ice to the North Atlantic (known as Heinrich events; these specific cold intervals are often referred to as *Heinrich stadials*). CO_2 decreases after a rapid switch to warmer conditions over Greenland (interstadials) and slower cooling in Antarctica (Bereiter et al., 2012). This strong relationship between Antarctic temperature and CO_2 has focused attention on the Southern Ocean (SO) as the major conduit for the transfer of carbon between the atmosphere and the ocean on millennial and glacial-interglacial timescales (Sigman et al., 2010), with possible triggers in the North Atlantic.

The ratios of carbon isotopes differ among key carbon reservoirs, and thus, some of the sources and sinks driving past atmospheric CO₂ can be constrained using the isotopic composition of atmospheric CO₂ (Bauska et al., 2016; Eggleston et al., 2016; Köhler et al., 2006; Schmitt et al., 2012). Four major processes fractionate the carbon isotopes ($\epsilon_{A-B} \cong \delta^{13}C_A - \delta^{13}C_B$): photosynthesis that makes CO₂ into organic carbon on land ($\epsilon_{\text{land-atmosphere}}$ = approximately -18%), photosynthesis in the surface ocean that forms particulate organic carbon from dissolved inorganic carbon ($\epsilon_{\text{POC-DIC}}$ = approximately -22%), air-sea gas exchange ($\epsilon_{\text{DIC-atmosphere}}$ = approximately $+8\%$; decreasing by 0.1% for every 1°C increase in ocean temperature), and a negligible fractionation during the formation of CaCO₃ in surface ocean ($\epsilon_{\text{DIC-CaCO}_3}$ = approximately 0%) by measuring the time varying changes in both atmospheric CO₂ concentrations and the $\delta^{13}C\text{-CO}_2$, we can constrain the sources of the CO₂ changes. Rising atmospheric CO₂ and decreasing $\delta^{13}C\text{-CO}_2$ is consistent with organic carbon sources to the atmosphere; rising atmospheric CO₂ and increasing $\delta^{13}C\text{-CO}_2$ is consistent with a warming ocean; and rising CO₂ with no changes in $\delta^{13}C\text{-CO}_2$ could indicate a balanced contribution of rising ocean temperature and organic carbon sources or the influence of CaCO₃ or volcanic sources. Air-sea gas exchange in the high-latitude ocean may affect atmospheric $\delta^{13}C\text{-CO}_2$, with rising atmospheric CO₂ and large decreases in $\delta^{13}C\text{-CO}_2$ predicted by box model experiments that include enhanced air-sea gas exchange in the SO (Bauska et al., 2016; Köhler et al., 2006). Finally, changes in the abundance of C3 and C4 plants on land (Ehleringer et al., 1997) or ecological shifts in marine biosphere (Broecker & McGee, 2013) would change the overall photosynthetic fractionation and thus the details, but not the fundamentals, of using $\delta^{13}C\text{-CO}_2$ to fingerprint carbon sources.

Other atmospheric gases provide additional constraints on carbon cycle variability, particularly related to the response of the terrestrial biosphere to abrupt climate change. Most evidence suggests that past variations in methane are dominated by climate variability over tropical and boreal wetlands (Brook et al., 2000; Rhodes et al., 2015). N₂O is produced in oxygen-poor ocean waters and terrestrial soils. Rising N₂O most likely reflects either decreasing oxygen levels in the intermediate-depth ocean, warmer terrestrial soil temperatures, or a combination of the two (Schilt et al., 2014). The $\delta^{18}O$ of atmospheric O₂ ($\delta^{18}O\text{-O}_2$) largely follows the changes in $\delta^{18}O$ of seawater and orbitally driven changes in the Dole effect, but rapid increases in $\delta^{18}O\text{-O}_2$ have been argued to reflect southward shifts in low-latitude precipitation (Seltzer et al., 2017; Severinghaus et al., 2009; see supporting information for definition of $\Delta\epsilon_{\text{LAND}}$).

2. Methods and Materials

We present new atmospheric histories of CO₂, N₂O, CH₄, and $\delta^{13}C\text{-CO}_2$ spanning 47–35 ka from the Taylor Glacier, Antarctica, blue ice area (Figures 1d–1g). The chronology (Baggenstos et al., 2017) is constructed by synchronizing the Taylor Glacier CH₄ and $\delta^{18}O\text{-O}_2$ records to the WAIS (West Antarctic Ice Sheet) Divide Ice Core (WDC) timescale (Buizert et al., 2015) and thus linking to the radiometrically dated Hulu Cave record (Cheng et al., 2016; Figure 1c). The concentrations of CO₂ and N₂O and the $\delta^{13}C\text{-CO}_2$ were measured on the same sample using the Oregon State University ice grater system (Bauska et al., 2014). The long-term reproducibility for CO₂, N₂O, and $\delta^{13}C\text{-CO}_2$ are ± 1 ppm, ± 5 ppb, and $+0.02\%$, respectively (Bauska et al., 2015, 2016). The combination of increased resolution and precision equates to a significant improvement over previous reconstructions which focused on longer-term changes (Eggleston et al., 2016; Figure S1). Additionally, previous reconstructions in this time interval were limited by offsets between cores (see Eggleston et al., 2016 for detailed discussion and Figure S2). Using the interval from 47 to 43 ka as a baseline for comparison, the Talos Dome $\delta^{13}C\text{-CO}_2$ record has significantly lower and more variable values (mean \pm s.d. = $-6.72 \pm 0.23\%$; $n = 12$) than data from the EPICA Dronning Maude Land ($-6.50 \pm 0.12\%$; $n = 8$) and EPICA Dome C ($-6.59 \pm 0.16\%$; $n = 5$) ice cores. In the same interval, the Taylor Glacier record averages $-6.55 \pm 0.07\%$ ($n = 14$) in broad agreement with EPICA Dronning Maude Land and EPICA Dome C. Although we can confidently interpret relative changes in our new record because of the improvement in precision and resolution, addressing the absolute accuracy of the $\delta^{13}C\text{-CO}_2$ values requires additional interlaboratory and intercore comparison.

3. Results

3.1. Ice Core Constraints on Greenhouse Gas Variability

The most salient mode of variability in atmospheric CO₂, the millennial-scale rising and falling with Antarctic temperature, is accompanied by an inversely correlated change in $\delta^{13}C\text{-CO}_2$ (Figures 1e and 1f). Atmospheric

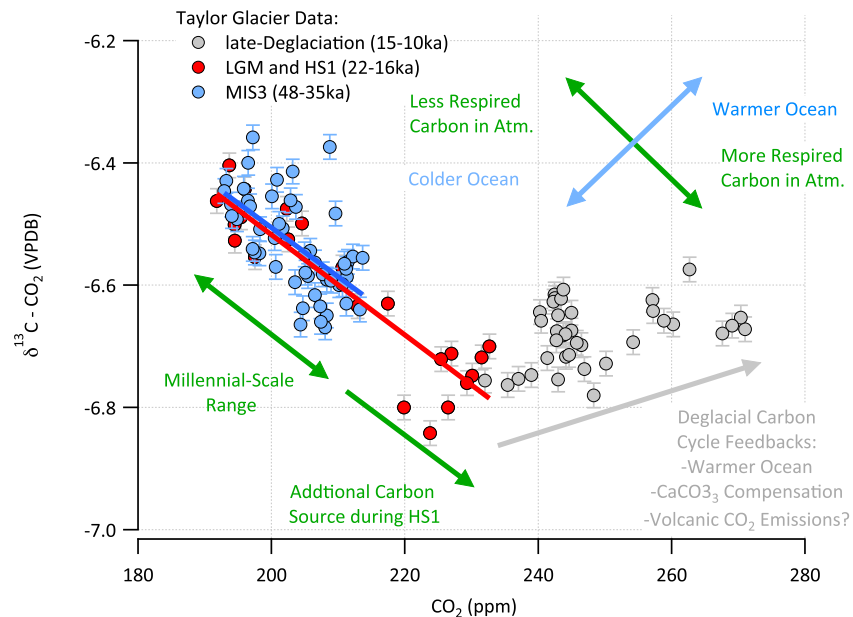


Figure 2. Cross-plot of atmospheric CO_2 and $\delta^{13}\text{C}\text{-CO}_2$ spanning the MIS3 section (blue, this study) and the last deglaciation, which is subdivided into the LGM to HS1 data (red) and late deglaciation (gray). Solid lines indicate linear regressions through the MIS3 (blue) and HS1 (red) data. MIS3 = Marine Isotope Stage 3; LGM = Last Glacial Maximum; HS = Heinrich stadial.

CO_2 ranges from about 195 to 215 ppm with the corresponding variability in $\delta^{13}\text{C}\text{-CO}_2$ spanning -6.45 to -6.65‰ (a -0.1‰ change for every $+10$ ppm). At finer scales, we observe several other modes of variability. The CO_2 rise during Heinrich stadial 4 (40.2–38.4 ka; *HS4*) starts off slowly, rising 3–4 ppm, while $\delta^{13}\text{C}\text{-CO}_2$ decreases by $\sim 0.05\text{‰}$. As noted previously in the Siple Dome ice core (Ahn & Brook, 2014), the rise then accelerates in a sharp jump of about 8 ppm. The rapid phase of the rise is coincident with the midstadial rise in CH_4 noted in the WAIS Divide Core (Rhodes et al., 2015; Figure 1d, red vertical line) and the increase in $\Delta\epsilon_{\text{LAND}}$ first observed in the Siple Dome Core (Severinghaus et al., 2009) and confirmed in the WDC record (Seltzer et al., 2017; Figure 1h). No change in N_2O is resolved in the Taylor Glacier data set, consistent with the Talos Dome record (Schilt et al., 2010; Figure 1g). The resolution of the carbon isotope measurements prevents a clear fingerprinting of the source but a replicated sample clearly falls to more negative values off the more gradual trend by about 0.1‰ (Figure 1f). In the later part of the HS4, CO_2 continues to rise slowly by 3 ppm and $\delta^{13}\text{C}\text{-CO}_2$ decreases by another 0.1‰ .

The onsets of DO interstadials are accompanied by small rises in CO_2 (Figure 1e, gray dashed lines). This variability has been noted in other cores and described as either a lagged response to Antarctic temperature (Bereiter et al., 2012) or, in the case of the weaker DO events, a lagged response to Greenland stadial conditions that are too short to impart a significant change in CO_2 (Ahn & Brook, 2014). In our record, we note that atmospheric CO_2 appears to increase along with CH_4 and N_2O with no discernable lead or lag. This is most prominent at DO8 when CH_4 rises by about 120 ppb, N_2O rises by 35 ppb, and CO_2 rises by 6 ppm (see also Figures 4n–4p). The other DO events (7, 9, and 10) are near the detection limit of our record and difficult to quantify. Across these events, $\delta^{13}\text{C}\text{-CO}_2$ either increases slightly ($\sim 0.08\text{‰}$ at DO8) or shows no substantial change.

4. Discussion

4.1. Millennial-Scale Carbon Cycle Variability

The overall negative correlation between CO_2 and $\delta^{13}\text{C}\text{-CO}_2$ rules out changes in ocean temperature, the CaCO_3 cycle, or volcanic input having a dominant role in driving millennial-scale CO_2 (Figure 2). Instead, the data are consistent with changes in terrestrial carbon storage or the strength of the ocean's

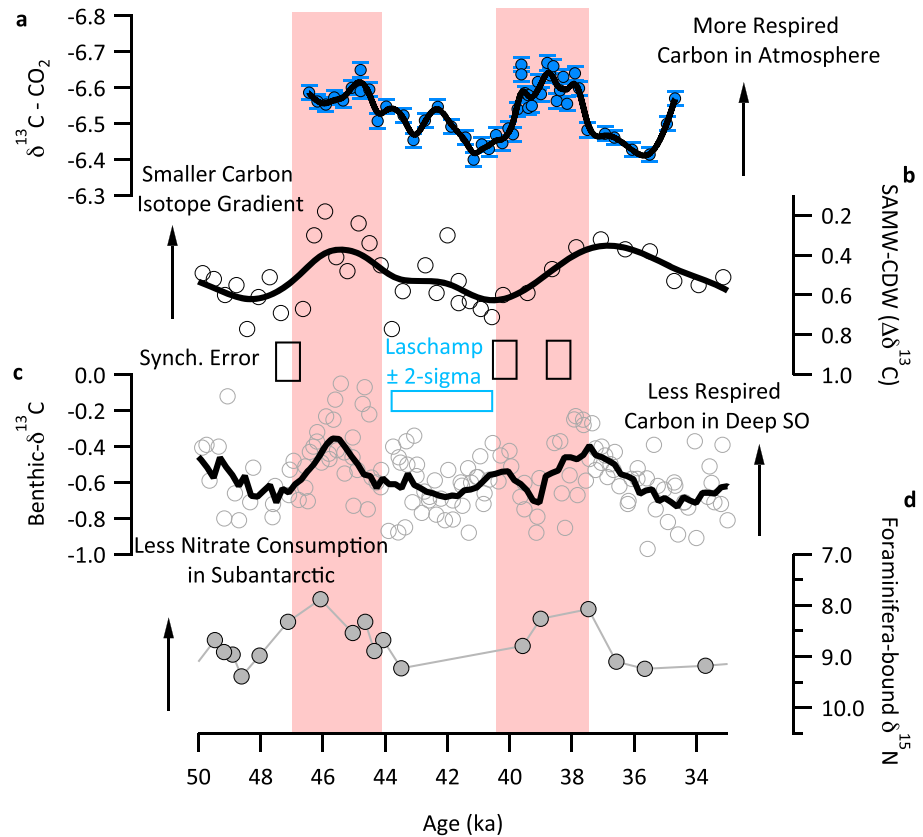


Figure 3. Comparison of atmospheric record of $\delta^{13}\text{C-CO}_2$ with oceanic records of $\delta^{13}\text{C}$ and nutrient utilization. (a) Atmospheric $\delta^{13}\text{C-CO}_2$ (this study) on an inverted y axis. (b) The difference in $\delta^{13}\text{C}$ between subantarctic mode water (SAMW) and circumpolar deepwater (CDW; Ziegler et al., 2013). A stack of benthic $\delta^{13}\text{C}$ (black line) from a combination of record in the deep Southern Ocean (SO; gray circles; Charles et al., 1996; Hodell et al., 2001, 2003; Ninnemann et al., 2004). Also indicated is the uncertainty on these chronologies (Barker & Diz, 2014) based on synchronization between carbonate preservation and Greenland temperature (black boxes) and independent age control based on the Laschamp event (blue boxes). (d) Foraminifera-bound $\delta^{15}\text{N}$ indicating nitrate consumption in sub-Antarctic (Martínez-García et al., 2014). Red bars highlight the broad millennia-scale correlations.

biological pump. If terrestrial sources were dominant, whole ocean $\delta^{13}\text{C}$ would follow atmospheric $\delta^{13}\text{C-CO}_2$. If oceanic sources from changes in the strength of the biological pump or shifts in ocean ventilation were dominant, the surface-to-deep gradient in $\delta^{13}\text{C}$ in inorganic carbon in the ocean would decrease along with atmospheric $\delta^{13}\text{C-CO}_2$.

Millennial-scale decreases in the vertical gradient of $\delta^{13}\text{C}$ in the SO have been tentatively correlated to maxima in atmospheric CO_2 (Charles et al., 2010; Ziegler et al., 2013) and, therefore, in light of our new data, minima in $\delta^{13}\text{C-CO}_2$ (Figures 3a and 3b). If this coupling of the oceanic gradient of $\delta^{13}\text{C}$ and atmospheric $\delta^{13}\text{C-CO}_2$ could be demonstrated to be precisely in-phase, it would provide clear evidence of an oceanic source controlling atmospheric CO_2 . Taking the current data and chronology at face value, the decreases in the oceanic $\delta^{13}\text{C}$ gradient are broadly associated with minima in atmospheric $\delta^{13}\text{C-CO}_2$, yet the coupling is clearly not one-to-one, possibly due to chronological errors in the marine sediment record. To explore this hypothesis further, we combined existing benthic carbon isotope records from deep SO (~42°S, 10°E, 4,600 m; Charles et al., 1996; Hodell et al., 2001, 2003; Ninnemann et al., 2004). These records use previously established age models that are tied to the Greenland ice core records using carbonate preservation and confirmed by ^{14}C data during the deglaciation and the Laschamp paleomagnetic event during MIS3 (~42 ka; Barker & Diz, 2014). We include a minor increase in the absolute age of 0.63% to account for the possible undercounting of annual layers in the Greenland Ice Core chronologies relative to the WDC timescale (Buizert et al., 2015).

We note that the atmosphere and deep ocean $\delta^{13}\text{C}$ are anticorrelated during MIS3 (Figure 3c). This supports the hypothesis that the waxing and waning of respired organic carbon source in the deep SO controlled atmospheric CO_2 and significantly limits the possibility of contributions from terrestrial sources. However, this relationship alone cannot delineate oceanic sources between changes in export productivity and changes in stratification. Evidence to support changes in export productivity comes from the correlation of the ice core data and foraminifera-bound $\delta^{15}\text{N}$ which indicates lower nitrate utilization during periods of high atmospheric CO_2 (Martínez-García et al., 2014; Figure 3d). Iron deposition rates and export production in the sub-Antarctic are also closely coupled, suggesting that the extent of iron limitation may have played a role in this enhanced nutrient utilization (Jaccard et al., 2016). Evidence in support of ventilation changes stems from radiocarbon constraints in the South Atlantic that are closely coupled with deep ocean oxygen levels, suggesting that both export productivity and ocean circulation were working in concert over this period (Gottschalk et al., 2016). A quantitative description of this coupling requires study with isotope-enabled Earth system models; however, additional insight can be gained by comparing to periods when these processes may have become uncoupled.

Our new high-resolution MIS3 data now provide a similar sequence of abrupt climate change events to contrast with the last deglaciation. First, we compare the MIS3 data to the last deglaciation utilizing a cross plot of CO_2 and $\delta^{13}\text{C}\text{-CO}_2$ (Figure 2). We see that the MIS3 data fall along the same trend observed during HS1 of the last deglaciation (~18–15.0 ka) yet only span about 50% of range (note that the low $\delta^{13}\text{C}\text{-CO}_2$ values that fall off this trend are due to centennial-scale variability at ~16.3 ka). This suggests that millennial-scale CO_2 variations in MIS3 can be linked mechanistically to the more pronounced variability during the deglaciation. As discussed in previous work, this covariability of CO_2 and $\delta^{13}\text{C}\text{-CO}_2$ is consistent with changes in SO ventilation (Köhler et al., 2006; Menviel, Mouchet, et al., 2015; Schmitt et al., 2012; Tschumi et al., 2011) changes in export production (particularly the SO; Bauska et al., 2016; Menviel et al., 2012) or a weakening of the ocean's biological pump by a reduction in North Atlantic Deep-water (NADW) formation (Schmittner & Lund, 2015).

Second, we compare the two intervals in time with the greenhouse gas records plotted over 8-ka intervals (Figures 4a–4c). Similar patterns of millennial-scale variability in CH_4 and N_2O are observed, but the changes in CO_2 appear fundamentally different. First, the CO_2 rise during HS1 is about 20 ppm greater than the rise in HS4 (or ~2 \times) and, second, CO_2 remains elevated after the switch to interstadial conditions during the Bølling-Allerød (BA) rather than decreasing as observed after the onset of DO8 (Figure 3c). The $\delta^{13}\text{C}\text{-CO}_2$ follows a similar pattern. In HS1, $\delta^{13}\text{C}\text{-CO}_2$ decreases by 0.2‰ more than HS4 and stabilizes during the BA as opposed to abrupt increases observed during DO8 (Figure 4d). What was different about the deglaciation that allowed more respired carbon into the atmosphere during HS1 than HS4 and prevented, or compensated for, a potential uptake of carbon during the BA?

During the Heinrich stadials, NADW weakens (Henry et al., 2016), and subantarctic productivity decreases (Anderson et al., 2014; Gottschalk et al., 2016) tracking dust delivery to Antarctica (Fischer et al., 2007; Figures 4e, 4h, and 4i). Ventilation of the SO (as inferred from radiocarbon) improves (Gottschalk et al., 2016; Skinner et al., 2010), and SO upwelling (as inferred from Antarctic productivity) increases (Anderson et al., 2009), although these changes could be more pronounced in the later part of the Heinrich stadials (Figures 4f and 4g). During MIS3, all of these changes are largely symmetric around, and consistent with, the minimum in $\delta^{13}\text{C}\text{-CO}_2$ and thus plausible drivers the change in CO_2 .

During the deglaciation, some variables trend back toward Last Glacial Maximum values after HS1 (NADW and SO upwelling), while others show near permanent shifts to interglacial levels during HS1 (subantarctic productivity and SO ventilation). This decoupling allows us to partially disentangle which processes control atmospheric CO_2 . Based on relationship between the proxies and atmospheric data in MIS3, we would expect that if changes in NADW and/or SO upwelling were to control atmospheric CO_2 , we would observe a large CO_2 decrease and $\delta^{13}\text{C}\text{-CO}_2$ increase in the BA. This is clearly not the case and requires either a muted response to these forcings or another source of carbon in the BA that compensated for the apparent carbon sink. Conversely, if changes in subantarctic productivity and SO ventilation dominated the atmospheric CO_2 budget, we could expect CO_2 to remain elevated during the BA and $\delta^{13}\text{C}\text{-CO}_2$ to plateau at lower values, a scenario that is in much better agreement with the data. Thus, subantarctic productivity and SO ventilation appear to have a more consistent link with atmospheric CO_2 in both MIS3 and the Last Deglaciation and are strong candidates for contributing significantly to glacial-interglacial CO_2 change.

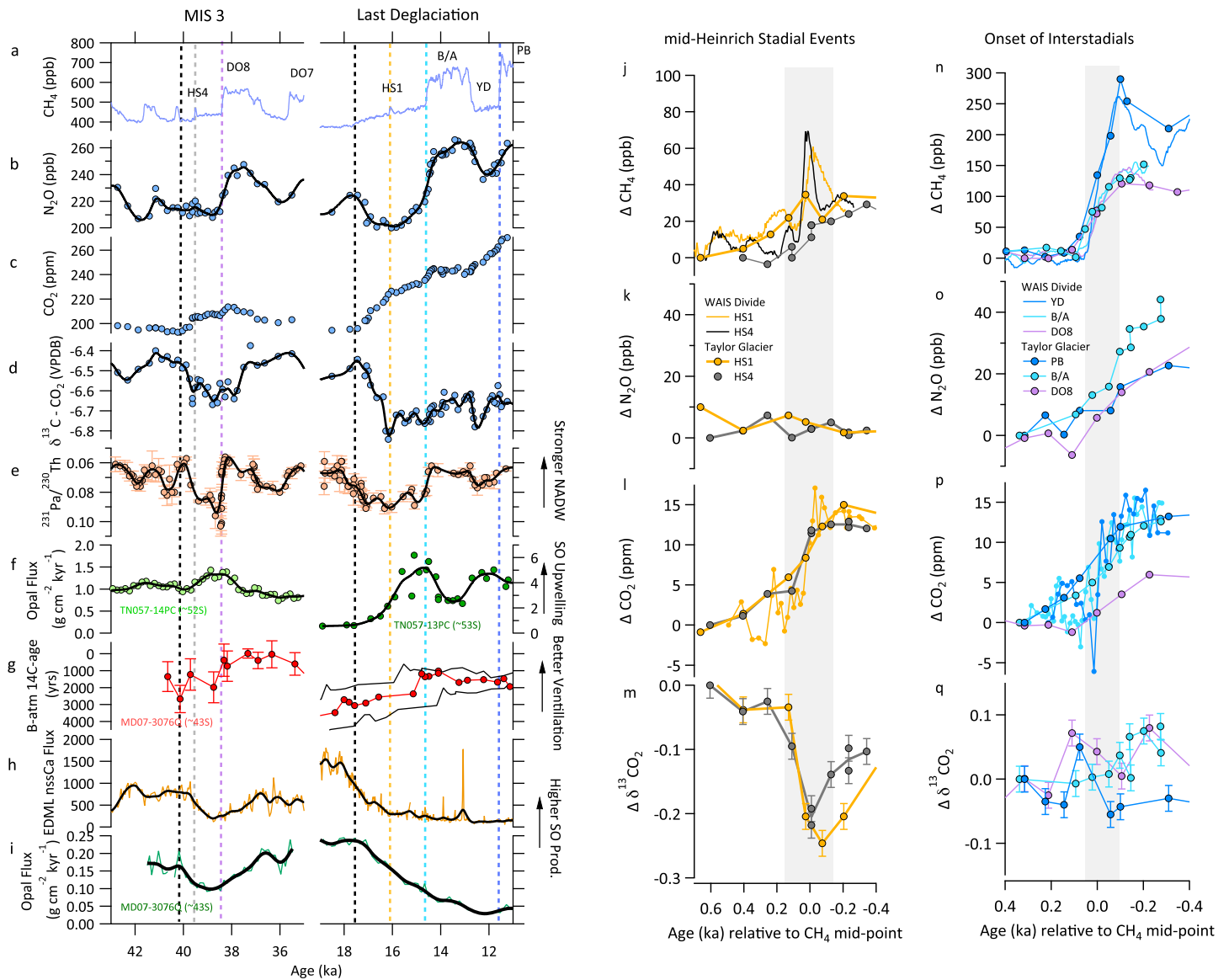


Figure 4. (left) Comparison of MIS3 data (this study) and last deglaciation (Bauska et al., 2016; Marcott et al., 2014; Rhodes et al., 2015) greenhouse gas variability. (a) WDC CH₄ (Rhodes et al., 2015). (b) Taylor Glacier N₂O. (c) Taylor glacier CO₂. (d) Taylor Glacier δ¹³C-CO₂. (e) Pa/Th, a proxy for the strength of NADW formation (Henry et al., 2016; McManus et al., 2004; orange), (f) the opal flux in the SO (Anderson et al., 2009), a proxy for upwelling (green; note the two different cores and axes are used in the comparison), (g) the benthic to atmosphere ¹⁴C age reconstructions for the subantarctic zone (Gottschalk et al., 2016; Skinner et al., 2010), (h) nssCa flux from the EDML ice core (Fischer et al., 2007), a proxy for dust delivery to Antarctica (brown), (i) opal flux in the subantarctic zone (Gottschalk et al., 2016), a proxy for productivity (from the same core as the ventilation reconstruction). Yellow and gray bars highlight the Heinrich Stadial jumps, black bars indicated the initial CO₂ rises, blue and purple bars highlight the onset of interstadials. (right) Centennial-scale variability during the last glacial period from Taylor glacier and WDC. Anomalies in the concentration and isotopic composition of the greenhouse gases are plotted with the relative timing determined by the midpoint in the CH₄ rise. Marker color corresponds to dashed lines in left panel. MIS3 = Marine Isotope Stage 3; NADW = North Atlantic Deep-water; SO = Southern Ocean; HS = Heinrich stadial; DO = Dansgaard-Oeschger.

4.2. Centennial-Scale Carbon Cycle Variability

On the centennial scale, our new observations in MIS3 can be combined with recently identified variability in Last Deglaciation to suggest a ubiquitous and consistent coupling of the carbon cycle with abrupt climate change events. In Figures 4j–4q, we plot variability in greenhouse gases for two categories of centennial-scale events: the onset of interstadials (DO8, the BA, and the preboreal) and mid-Heinrich stadials events (HS4 and HS1). The changes are plotted as anomalies, and the timing is set relative to the midpoint of the rise in CH₄. Note that the Taylor Glacier chronology is synchronized with the WAIS Divide record via CH₄, and thus, the phasing of the two ice cores cannot be interpreted.

The rapid 8-ppm CO₂ rise during HS4 at 39.5 ka likely shares a common origin with a similar event during the deglaciation with HS1 at 16.3 ka (Marcott et al., 2014; Figure 4l). Both events are associated with carbon isotope minima (Figure 4m). It has been suggested that these midstadial events can be tied to the timing of the Heinrich events and may represent a rapid release of terrestrial carbon to the atmosphere driven by a cooling and drying of the Northern Hemisphere (Bauska et al., 2016). The event in HS4 is consistent with a terrestrial origin as it coincides with an increase in CH₄ (Rhodes et al., 2015; Figure 4j), which may indicate enhanced precipitation of the Southern Hemisphere tropics, and an increase in $\Delta\epsilon_{\text{LAND}}$, which suggests decreased precipitation in the Northern Hemisphere (Seltzer et al., 2017; Severinghaus et al., 2009; Figure 1h). Constant N₂O indicates either that changes in terrestrial soil temperatures may have been small on the global scale, thus suggesting that precipitation was the dominant driver of the terrestrial carbon loss, or that oxygen-minimum zones in intermediate ocean were relatively stable, possibly indicating the absence of a change in ocean circulation across this event (Figure 4k).

The 6-ppm CO₂ rise at the onset of DO8 shares common features with the onset of the BA and preboreal (~11.5 ka) during the deglaciation (Figure 4p). All three events exhibit simultaneous increases in CO₂, CH₄, and N₂O that coincide with abrupt Northern Hemisphere warmings, continued warming, or at least stable temperatures in Antarctica (WAIS Divide Project Members, 2015) and greater NADW formation (Henry et al., 2016; McManus et al., 2004). The $\delta^{13}\text{C-CO}_2$ across all events is variable but shows no secular trend (preboreal) or slight increase of ~0.08‰ (BA and DO8; Figure 4q). At face value, this pattern of increasing CO₂ and increasing $\delta^{13}\text{C-CO}_2$ indicates that rising ocean temperature contributed to the CO₂ rise with additional (but limited) changes in the net flux of organic carbon. This simplest of scenarios is somewhat surprising given that changes in the ocean's biological pump may accompany the large and abrupt reorganization of ocean circulation, and changes in terrestrial carbon reservoirs are clearly indicated by the large increases in CH₄ and N₂O. Recently, the LOVECLIM model, which predicts a small positive relationship between CO₂ and $\delta^{13}\text{C-CO}_2$ during reduced NADW (Menviel, Spence, et al., 2015), also predicts increases in CO₂ of 10 to 15 ppm upon the resumption of NADW (with the effect of solubility contributing about 50% to CO₂ variability; Menviel, Mouchet, et al., 2015). Moreover, a precisely dated coral record shows that these events during the last deglaciation are associated with brief intervals of enhanced overturning in the Atlantic (Chen et al., 2015). This integrated response to the onset of an interstadial is consistent with the CO₂ and $\delta^{13}\text{C-CO}_2$ data and may be a pervasive feature of last glacial period CO₂ variability but requires ground-truthing with additional, high-resolution MIS3 marine records.

5. Conclusions

Carbon isotope data from the last deglaciation and last glacial period clearly show that CO₂ variability is the sum of multiple mechanisms, many of which are triggered by abrupt climate change. During both periods, millennial-scale variability is present and likely associated with the release of respired organic carbon from the deep ocean. Superimposed on these oscillations are two types of centennial-scale changes, (i) CO₂ increases and $\delta^{13}\text{C-CO}_2$ decreases in the middle of Heinrich stadials and (ii) CO₂ increases and small changes in $\delta^{13}\text{C-CO}_2$ that are in-phase with rapid increases in NH temperature. During the deglaciation, the millennial-scale component is enhanced, and an additional carbon source is required to sustain the CO₂ rise through the entire deglaciation. This suggests that although abrupt climate variability is not the sole driver of the deglacial CO₂ rise, it may be a prerequisite. These potential links can now be tested with model experiments that use the MIS3 data to constrain the sensitivity to centennial and millennial-scale components and the deglacial data to evaluate how these mechanisms interact with changes in insolation, ice volume, and global temperatures.

Acknowledgments

This work was funded by NSF grants ANT 0838936 (Oregon State University) and ANT 0839031 (Scripps Institution of Oceanography). Data will be made available online at National Climate Data Center (<https://www.ncdc.noaa.gov/paleo/study/24170>).

References

- Ahn, J., & Brook, E. J. (2008). Atmospheric CO₂ and climate on millennial time scales during the last glacial period. *Science*, 322(5898), 83–85. <https://doi.org/10.1126/science.1160832>
- Ahn, J., & Brook, E. J. (2014). Siple dome ice reveals two modes of millennial CO₂ change during the last ice age. *Nature Communications*, 5(3723), 1. <https://doi.org/10.1038/ncomms4723>
- Anderson, R. F., Ali, S., Bradtmiller, L. I., Nielsen, S. H. H., Fleisher, M. Q., Anderson, B. E., & Burckle, L. H. (2009). Wind-driven upwelling in the Southern Ocean and the Deglacial rise in atmospheric CO₂. *Science*, 323(5920), 1443–1448. <https://doi.org/10.1126/science.1167441>

- Anderson, R. F., Barker, S., Fleisher, M., Gersonde, R., Goldstein, S. L., Kuhn, G., et al. (2014). Biological response to millennial variability of dust and nutrient supply in the subantarctic South Atlantic Ocean. *Philosophical Transactions of the Royal Society of London A: Mathematical, Physical and Engineering Sciences*, 372(2019), 20130054. <https://doi.org/10.1098/rsta.2013.0054>
- Baggenstos, D., Bauska, T. K., Severinghaus, J. P., Lee, J. E., Schaefer, H., Buizert, C., et al. (2017). Atmospheric gas records from Taylor Glacier, Antarctica, reveal ancient ice with ages spanning the entire last glacial cycle. *Climate of the Past*, 13(7), 943–958. <https://doi.org/10.5194/cp-13-943-2017>
- Barker, S., & Diz, P. (2014). Timing of the descent into the last ice age determined by the bipolar seesaw. *Paleoceanography*, 29, 489–507. <https://doi.org/10.1002/2014PA002623>
- Bauska, T. K., Baggenstos, D., Brook, E. J., Mix, A. C., Marcott, S. A., Petrenko, V. V., et al. (2016). Carbon isotopes characterize rapid changes in atmospheric carbon dioxide during the last deglaciation. *Proceedings of the National Academy of Sciences*, 113(13), 3465–3470. <https://doi.org/10.1073/pnas.1513868113>
- Bauska, T. K., Brook, E. J., Mix, A. C., & Ross, A. (2014). High-precision dual-inlet IRMS measurements of the stable isotopes of CO₂ and the N₂O/CO₂ ratio from polar ice core samples. *Atmospheric Measurement Techniques*, 7(11), 3825–3837. <https://doi.org/10.5194/amt-7-3825-2014>
- Bauska, T. K., Joos, F., Mix, A. C., Roth, R., Ahn, J., & Brook, E. J. (2015). Links between atmospheric carbon dioxide, the land carbon reservoir and climate over the past millennium. *Nature Geoscience*, 8(5), 383–387. <https://doi.org/10.1038/ngeo2422>
- Bereiter, B., Lüthi, D., Siegrist, M., Schüpbach, S., Stocker, T. F., & Fischer, H. (2012). Mode change of millennial CO₂ variability during the last glacial cycle associated with a bipolar marine carbon seesaw. *Proceedings of the National Academy of Sciences*, 109(25), 9755–9760. <https://doi.org/10.1073/pnas.1204069109>
- Broecker, W. S., & McGee, D. (2013). The ¹³C record for atmospheric CO₂: What is it trying to tell us? *Earth and Planetary Science Letters*, 368(0), 175–182. <https://doi.org/10.1016/j.epsl.2013.02.029>
- Brook, E. J., Harder, S., Severinghaus, J., Steig, E. J., & Sucher, C. M. (2000). On the origin and timing of rapid changes in atmospheric methane during the last glacial period. *Global Biogeochemical Cycles*, 14(2), 559–572. <https://doi.org/10.1029/1999GB001182>
- Buizert, C., Cuffey, K. M., Severinghaus, J. P., Baggenstos, D., Fudge, T. J., Steig, E. J., et al. (2015). The WAIS divide deep ice core WD2014 chronology—Part 1: Methane synchronization (68–31 ka BP) and the gas age–ice age difference. *Climate of the Past*, 11(2), 153–173. <https://doi.org/10.5194/cp-11-153-2015>
- Charles, C. D., Lynch-Stieglitz, J., Ninnemann, U. S., & Fairbanks, R. G. (1996). Climate connections between the hemisphere revealed by deep sea sediment core/ice core correlations. *Earth and Planetary Science Letters*, 142(1–2), 19–27. [https://doi.org/10.1016/0012-821X\(96\)00083-0](https://doi.org/10.1016/0012-821X(96)00083-0)
- Charles, C. D., Pahnke, K., Zahn, R., Mortyn, P. G., Ninnemann, U., & Hodell, D. A. (2010). Millennial scale evolution of the Southern Ocean chemical divide. *Quaternary Science Reviews*, 29(3–4), 399–409. <https://doi.org/10.1016/j.quascirev.2009.09.021>
- Chen, T., Robinson, L. F., Burke, A., Southon, J., Spooner, P., Morris, P. J., & Ng, H. C. (2015). Synchronous centennial abrupt events in the ocean and atmosphere during the last deglaciation. *Science*, 349(6255), 1537–1541. <https://doi.org/10.1126/science.aac6159>
- Cheng, H., Edwards, R. L., Sinha, A., Spötl, C., Yi, L., Chen, S., et al. (2016). The Asian monsoon over the past 640,000 years and ice age terminations. *Nature*, 534(7609), 640–646. <https://doi.org/10.1038/nature18591>
- Clark, P. U., Shakun, J. D., Marcott, S. A., Mix, A. C., Eby, M., Kulp, S., et al. (2016). Consequences of twenty-first-century policy for multi-millennial climate and sea-level change. *Nature Climate Change*, 6(4), 360–369. <https://doi.org/10.1038/nclimate2923>
- Eggleson, S., Schmitt, J., Bereiter, B., Schneider, R., & Fischer, H. (2016). Evolution of the stable carbon isotope composition of atmospheric CO₂ over the last glacial cycle. *Paleoceanography*, 31, 434–452. <https://doi.org/10.1002/2015PA002874>
- Ehleringer, J. R., Cerling, T. E., & Helliker, B. R. (1997). C4 photosynthesis, atmospheric CO₂, and climate. *Oecologia*, 112(3), 285–299. <https://doi.org/10.1007/s004420050311>
- Fischer, H., Fundel, F., Ruth, U., Twarloh, B., Wegner, A., Udisti, R., et al. (2007). Reconstruction of millennial changes in dust emission, transport and regional sea ice coverage using the deep EPICA ice cores from the Atlantic and Indian Ocean sector of Antarctica. *Earth and Planetary Science Letters*, 260(1–2), 340–354. <https://doi.org/10.1016/j.epsl.2007.06.014>
- Gottschalk, J., Skinner, L. C., Lippold, J., Vogel, H., Frank, N., Jaccard, S. L., & Waelbroeck, C. (2016). Biological and physical controls in the Southern Ocean on past millennial-scale atmospheric CO₂ changes. *Nature Communications*, 7, 11539. <https://doi.org/10.1038/ncomms11539>
- Henry, L. G., McManus, J. F., Curry, W. B., Roberts, N. L., Piotrowski, A. M., & Keigwin, L. D. (2016). North Atlantic Ocean circulation and abrupt climate change during the last glaciation. *Science*, 353(6298), 470–474. <https://doi.org/10.1126/science.aaf5529>
- Hodell, D. A., Kanfoush, S. L., Shemesh, A., Crosta, X., Charles, C. D., & Guilderson, T. P. (2001). Abrupt cooling of Antarctic surface waters and sea ice expansion in the South Atlantic sector of the Southern Ocean at 5000 cal yr B.P. *Quaternary Research*, 56(02), 191–198. <https://doi.org/10.1006/qres.2001.2252>
- Hodell, D. A., Venz, K. A., Charles, C. D., & Ninnemann, U. S. (2003). Pleistocene vertical carbon isotope and carbonate gradients in the South Atlantic sector of the Southern Ocean. *Geochemistry, Geophysics, Geosystems*, 4(1), 1004. <https://doi.org/10.1029/2002GC000367>
- Indermuhle, A., Wahlen, M., Monnin, E., Stauffer, B., & Stocker, T. F. (2000). Atmospheric CO₂ concentration from 60 to 20 kyr BP from the Taylor dome ice core, Antarctica. *Geophysical Research Letters*, 27(5), 735–738. <https://doi.org/10.1029/1999GL010960>
- Jaccard, S. L., Galbraith, E. D., Martínez-García, A., & Anderson, R. F. (2016). Covariation of deep Southern Ocean oxygenation and atmospheric CO₂ through the last ice age. *Nature*, 530(7589), 207–210. <https://doi.org/10.1038/nature16514>
- Köhler, P., Fischer, H., Schmitt, J., & Munhoven, G. (2006). On the application and interpretation of keeling plots in paleo climate research—deciphering delta C-13 of atmospheric CO₂ measured in ice cores. *Biogeosciences*, 3(4), 539–556. <https://doi.org/10.5194/bg-3-539-2006>
- Marcott, S. A., Bauska, T. K., Buizert, C., Steig, E. J., Rosen, J. L., Cuffey, K. M., et al. (2014). Centennial-scale changes in the global carbon cycle during the last deglaciation. *Nature*, 514(7524), 616–619. <https://doi.org/10.1038/nature13799>
- Martínez-García, A., Sigman, D. M., Ren, H., Anderson, R. F., Straub, M., Hodell, D. A., et al. (2014). Iron fertilization of the Subantarctic Ocean during the last ice age. *Science*, 343(6177), 1347. <https://doi.org/10.1126/science.1246848>
- McManus, J. F., Francois, R., Gherardi, J. M., Keigwin, L. D., & Brown-Leger, S. (2004). Collapse and rapid resumption of Atlantic meridional circulation linked to deglacial climate changes. *Nature*, 428(6985), 834–837. <https://doi.org/10.1038/nature02494>
- Menviel, L., Joos, F., & Ritz, S. P. (2012). Simulating atmospheric CO₂, ¹³C and the marine carbon cycle during the last glacial–interglacial cycle: Possible role for a deepening of the mean remineralization depth and an increase in the oceanic nutrient inventory. *Quaternary Science Reviews*, 56, 46–68. <https://doi.org/10.1016/j.quascirev.2012.09.012>
- Menviel, L., Spence, P., & England, M. H. (2015). Contribution of enhanced Antarctic bottom water formation to Antarctic warm events and millennial-scale atmospheric CO₂ increase. *Earth and Planetary Science Letters*, 413, 37–50. <https://doi.org/10.1016/j.epsl.2014.12.050>
- Menviel, L., Mouchet, A., Meissner, K., Joos, F., & England, M. (2015). Impact of oceanic circulation changes on atmospheric δ¹³C. *Global Biogeochemical Cycles*, 29, 1944–1961. <https://doi.org/10.1002/2015GB005207>

- Ninnemann, U. S., Charles, C. D., & Hodell, D. A. (1999). Origin of Global Millennial Scale Climate Events: Constraints from the Southern Ocean deep sea sedimentary record. In *mechanisms of global climate change at millennial time scales* (pp. 99–112). Washington, DC: American Geophysical Union. <https://doi.org/10.1029/GM112p0099>
- North Greenland Ice Core Project Members (2004). High-resolution record of Northern Hemisphere climate extending into the last interglacial period. *Nature*, *431*(7005), 147–151.
- Rhodes, R. H., Brook, E. J., Chiang, J. C. H., Blunier, T., Maselli, O. J., McConnell, J. R., et al. (2015). Enhanced tropical methane production in response to iceberg discharge in the North Atlantic. *Science*, *348*(6238), 1016–1019. <https://doi.org/10.1126/science.1262005>
- Schilt, A., Baumgartner, M., Schwander, J., Buiron, D., Capron, E., Chappellaz, J., et al. (2010). Atmospheric nitrous oxide during the last 140,000 years. *Earth and Planetary Science Letters*, *300*(1–2), 33–43. <https://doi.org/10.1016/j.epsl.2010.09.027>
- Schilt, A., Brook, E. J., Bauska, T. K., Baggenstos, D., Fischer, H., Joos, F., et al. (2014). Isotopic constraints on marine and terrestrial N₂O emissions during the last deglaciation. *Nature*, *516*(7530), 234–237.
- Schmitt, J., Schneider, R., Elsig, J., Leuenberger, D., Laurantou, A., Chappellaz, J., et al. (2012). Carbon isotope constraints on the deglacial CO₂ rise from ice cores. *Science*, *336*(6082), 711–714. <https://doi.org/10.1126/science.1217161>
- Schmittner, A., & Lund, D. C. (2015). Early deglacial Atlantic overturning decline and its role in atmospheric CO₂ rise inferred from carbon isotopes ($\delta^{13}\text{C}$). *Climate of the Past*, *11*(2), 135–152. <https://doi.org/10.5194/cp-11-135-2015>
- Seltzer, A. M., Buizert, C., Baggenstos, D., Brook, E. J., Ahn, J., Yang, J.-W., & Severinghaus, J. P. (2017). Does $\delta^{18}\text{O}$ of O₂ record meridional shifts in tropical rainfall? *Climate of the Past*, *13*(10), 1323–1338. <https://doi.org/10.5194/cp-13-1323-2017>
- Severinghaus, J. P., Beaudette, R., Headly, M. A., Taylor, K., & Brook, E. J. (2009). Oxygen-18 of O₂ records the impact of abrupt climate change on the terrestrial biosphere. *Science*, *324*(5933), 1431–1434. <https://doi.org/10.1126/science.1169473>
- Sigman, D. M., Hain, M. P., & Haug, G. H. (2010). The polar ocean and glacial cycles in atmospheric CO₂ concentration. *Nature*, *466*(7302), 47–55. <https://doi.org/10.1038/nature09149>
- Skinner, L. C., Fallon, S., Waelbroeck, C., Michel, E., & Barker, S. (2010). Ventilation of the deep Southern Ocean and deglacial CO₂ rise. *Science*, *328*(5982), 1147–1151. <https://doi.org/10.1126/science.1183627>
- Tschumi, T., Joos, F., Gehlen, M., & Heinze, C. (2011). Deep ocean ventilation, carbon isotopes, marine sedimentation and the deglacial CO₂ rise. *Climate of the Past*, *7*(3), 771–800. <https://doi.org/10.5194/cp-7-771-2011>
- WAIS Divide Project Members (2015). Precise inter-polar phasing of abrupt climate change during the last ice age. *Nature*, *520*(7549), 661–665.
- Ziegler, M., Diz, P., Hall, I. R., & Zahn, R. (2013). Millennial-scale changes in atmospheric CO₂ levels linked to the Southern Ocean carbon isotope gradient and dust flux. *Nature Geoscience*, *6*(6), 457–461. <https://doi.org/10.1038/ngeo1782>